frontiers | Frontiers in Computer Science

TYPE Original Research
PUBLISHED 10 June 2024
DOI 10.3389/fcomp.2024.1406086

OPEN ACCESS

EDITED BY
Fiona Maree Chatteur,
Torrens University Australia, Australia

REVIEWED BY
Praveen Kumar Balachandran,
Vardhaman College of Engineering, India
Shahzad Ashraf,
NFC Institute of Engineering and Technology (NFCIET), Pakistan

*CORRESPONDENCE
Hong Qin
✉ Hong-Qin@utc.edu
Saurav Mallik
✉ sauravmtech2@gmail.com
Abhilash Pati
✉ er.abhilash.pati@gmail.com
Jayant Giri
✉ jayantpgiri@gmail.com
Murthy Cherukuri
✉ chmurthy2007@gmail.com

RECEIVED 24 March 2024
ACCEPTED 17 May 2024
PUBLISHED 10 June 2024

CITATION
Swain K, Cherukuri M, Samanta IS, Pati A, Giri J, Panigrahi A, Qin H and Mallik S (2024) Fuzzy Markov model for the reliability analysis of hybrid microgrids.
Front. Comput. Sci. 6:1406086.
doi: 10.3389/fcomp.2024.1406086

Fuzzy Markov model for the reliability analysis of hybrid microgrids

Kunjabihari Swain[1], Murthy Cherukuri[1]*, Indu Sekhar Samanta[2], Abhilash Pati[2]*, Jayant Giri [3,4]*, Amrutanshu Panigrahi[2], Hong Qin[5]* and Saurav Mallik[6]*

[1]Department of Electrical and Electronics Engineering, NIST University, Berhampur, India, [2]Department of Computer Science and Engineering, Siksha 'O' Anusandhan (Deemed to be University), Bhubaneswar, India, [3]Department of Mechanical Engineering, Yeshwantrao Chavan College of Engineering, Nagpur, India, [4]Department of VLSI Microelectronics, Saveetha School of Engineering, Saveetha Institute of Medical and Technical Sciences (SIMATS), Saveetha University, Chennai, India, [5]Department of Computer Science and Engineering, University of Tennessee at Chattanooga, Chattanooga, TN, United States, [6]Department of Environmental Health, Harvard T.H. Chan School of Public Health, Boston, MA, United States

This research presents a process for analyzing a hybrid microgrid's dependability using a fuzzy Markov model. The research initiated an analysis of the various microgrid components, such as wind power systems, solar photovoltaic (PV) systems, and battery storage systems. The states that are induced by component failures are represented using a state-space model. The research continues by suggesting a hybrid microgrid reliability model that analyzes data using a Markov process. Problems arise when trying to estimate reliability metrics for the microgrid using data that is both restricted and imprecise. This is why the study takes uncertainties into account to make microgrid reliability estimations more realistic. The importance of microgrid components concerning their overall availability is evaluated using fuzzy sets and reliability assessments. The study uses numerical analysis and then carefully considers the outcomes. The overall availability of hybrid microgrids is 0.99999.

KEYWORDS

microgrid, fuzzy Markov model, reliability analysis, wind, solar, battery

1 Introduction

Due to its versatile operational modes, encompassing grid-connected, and islanded configurations, microgrids are increasingly pivotal in establishing resilient electrical energy networks, especially in the face of natural disasters and adverse conditions. Typically incorporating distributed generation facilities capable of supplying heat and electricity, microgrids are anticipated to witness substantial integration of renewable energy sources. They constitute a fundamental component of smart grids (Nikos, 2007; Ashraf et al., 2020).

Reliability, defined as the capacity of an entity to fulfill a specified function within predetermined environmental and operational parameters and for a defined duration (Billinton and Allan, 1992), is of paramount importance in the context of microgrid systems. This significance arises from their role as backup power systems, particularly during main grid blackouts or failures. An in-depth examination of microgrid system reliability is crucial for system design and maintenance. Such an analysis offers insights into potential failure modes of subsystems and components, catering to the informational needs of system designers, operators, and end-users. Furthermore, it facilitates the estimation of the system's operational lifespan by predicting the time elapsed before the occurrence of the microgrid's initial physical failure. Consequently, reliability analysis emerges as a critical undertaking during the design and operational phases of microgrid implementation.

In the study by Said et al. (2019), a new SMES controller based on the fuzzy logic control method is presented, considering the state of charge of the superconducting magnetic energy storage (SMES) system to enhance its reliability. This controller effectively avoids the short-lifetime shortcoming of SMES and maintains constant bus voltages despite the fluctuating power of PV generation, thereby improving the overall microgrid system's reliability. Additionally, the proposed controller design method can be generalized for different microgrid architectures, offering a versatile solution for enhancing microgrid reliability. Akbari and Hesamian (2020) presented a method for constructing time-dependent reliability systems based on intuitionistic fuzzy random variables. The reliability functions of a k-out-of-n system are evaluated using an intuitionistic fuzzy random variable with exact parameters. The evaluation criteria are discussed and interpreted. Numerical evaluations are presented to illustrate the calculation of the system reliability criteria in the form of intuitionistic fuzzy numbers. In the study by Kumar et al. (2021), the authors presented the fuzzy reliability of a specific system utilizing intuitionistic fuzzy set theory and the universal generating function technique. The analysis relies on triangular fuzzy numbers and exponential distribution in lower and upper forms. In the study by Talaat et al. (2023), the authors provided a comprehensive review of the challenges and potential solutions for integrating renewable energy sources into microgrids. It highlights the role of artificial intelligence (AI) in improving integration and control strategies. It presents case studies on using AI to optimize the performance of hybrid renewable energy systems. Overall, this file offers valuable insights for researchers and practitioners working in the field of renewable energy integration. In the study by Ren et al. (2020), the authors developed a reliability model for radial multi-microgrids using the Bayesian network considering distribution network transmission capacity. A reliability assessment of aggregate battery energy storage systems in microgrids was proposed by Pham et al. (2020) using the Markov model. In the study by Kwasinski et al. (2012), the authors addressed the availability of microgrids during natural disasters. Microgrid availability is evaluated using the Markov model and evaluated using minimal cut set approximations. In the study by Ahshan et al. (2017), the authors have built a microgrid reliability model that takes into account the intermittent effects of renewable energy sources such as wind using Monte Carlo simulation. Adefarati and Bansal (2019) relied on the assessment of the reliability and economic and environmental advantages of renewable energy sources in the microgrid system. In the study by Ansari et al. (2016), the authors assessed the reliability of microgrids containing prioritized loads and distributed renewable energy resources through a hybrid analytical simulation method. Xu et al. (2016) focused on assessing the reliability of the microgrid accurately, taking into account its operating condition. A reliability assessment of the microgrid consisting of conventional generators, a photovoltaic system, and a small hydropower plant based on Monte Carlo simulation was presented (Na and Kim, 2019). In the study by Santhan et al. (2022), the authors introduced a method to enhance the resilience of existing microgrids against low-probability, high-impact events using Monte Carlo simulation and load prioritization. It evaluates this approach by modeling the IEEE 5-Bus and IEEE 14-Bus systems, assessing the impact of load shedding on microgrid resilience across different grid sizes, and introducing a new resilience index. Khare and Chaturvedi (2023) presented a thorough evaluation of microgrid systems, covering optimal design considerations and control system evaluation, and drew insights from a detailed analysis of literature and case studies. Khalili et al. (2022) introduced a novel approach to optimizing the power scheduling of energy sources in an isolated microgrid, focusing on the upside risk for the first time. The microgrid under consideration includes diverse sources such as wind turbines, photovoltaic panels, diesel generators, and batteries. Onaolapo and Ojo (2023) emphasize the importance of microgrids in balancing power consumption and generation, thus enhancing customer satisfaction and addressing challenges posed by events such as COVID-19.

The above reliability models are such that the transition rates of reliability are treated as crisp numbers. Input parameters such as failure rates and repair rates have been extracted from historical documents that may be prone to errors in reliability assessment methods. Due to the probabilistic characteristics of failure situations and variations in the environment, these parameters reveal considerable unit-to-unit variability.

Presuming a probability distribution for input parameters and utilizing either the conditional probability method by Billinton and Allan (1992) or the Monte Carlo simulation by Li (2013) are two traditional methods to integrate such uncertainties. However, identifying appropriate probability distributions in most situations proves challenging. Furthermore, the computational demands of traditional probabilistic methods could be substantial, particularly for expansive systems. In reliability analyses, methodologies based on fuzzy sets should specifically consider the uncertainties of input parameters (Klir and Yuan, 1996). Instead of single-point output, they can also generate possibility distributions. In addition, a subjective collection of information evaluated by expert opinions may be considered in such applications (Bowles and Pelaez, 1995; Kabir and Papadopoulos, 2018).

The reliability data for a device can be determined either by relating statistical methods to historical data or by using the reliability modeling of the device as a single system. The proposed work deals with a reliability model for hybrid microgrids. A reliability model for a hybrid microgrid was proposed by Adefarati and Bansal (2017), in which reliability transition rates were considered crisp numbers. In reliability evaluation methods, input parameters such as failure and repair rates were derived from historical records, which are prone to errors. Furthermore, due to the stochastic character of both ecological changes and failure situations, these metrics exhibit significant variability from one unit to the next. The true and single-point values of these parameters could lead to errors in reliability evaluations. Thus, fuzzy sets are taken into account for reliability analysis to integrate the inherent uncertainties associated with the input data.

This study focuses on the reliability modeling of a hybrid microgrid through the application of a fuzzy Markov model. Initially, comprehensive descriptions of microgrid components and their functionalities are provided, followed by the development of a state-space reliability model. The availability of the microgrid is subsequently computed based on the formulated model.

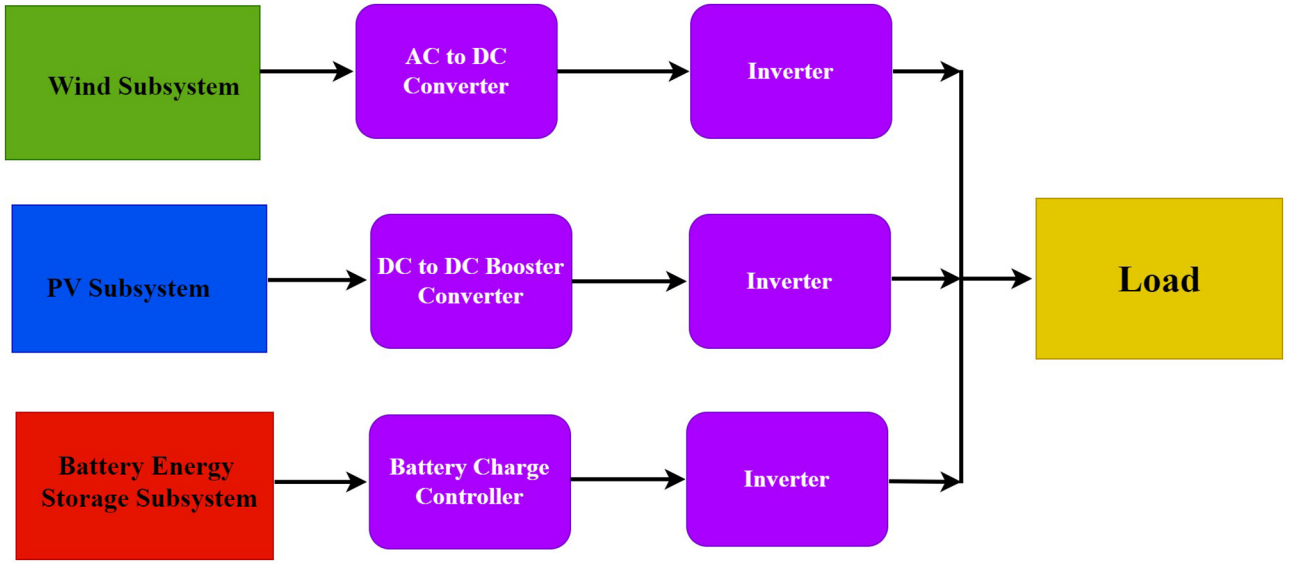

FIGURE 1
Hybrid microgrid.

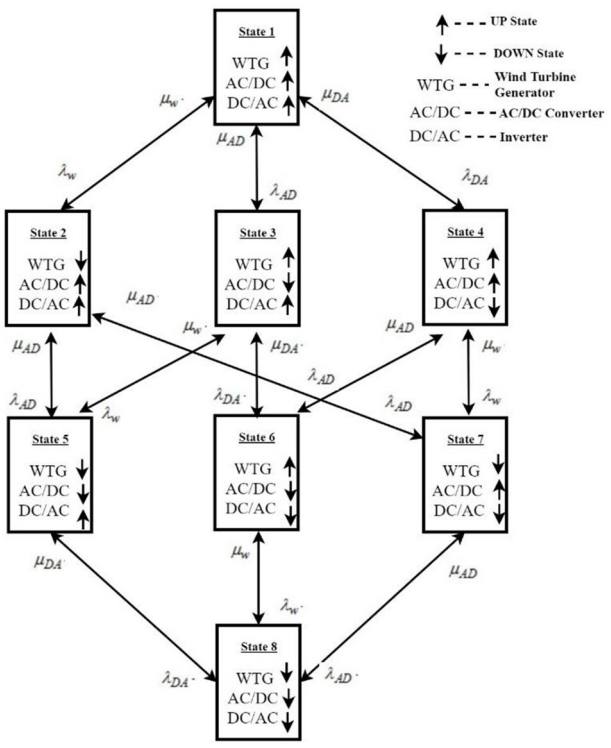

FIGURE 2
Eight-state Markov model of wind subsystem.

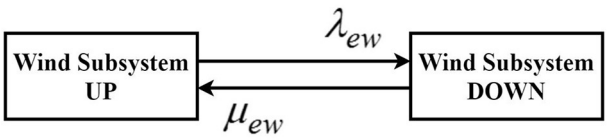

FIGURE 3
Equivalent two-state Markov model of wind subsystem.

The integration of fuzzy sets is employed in the reliability analysis to account for uncertainties inherent in the input data. Numerical illustrations are systematically studied to assess the efficacy of the suggested framework. The utility of the suggested framework extends to microgrid manufacturers, offering a tool for discerning critical microgrid components. This insight enables manufacturers to optimize investments in microgrid components, thereby enhancing overall microgrid availability.

The subsequent segments of this article are structured as follows. Section 2 provides a concise discourse on the constituent elements of a microgrid. The reliability modeling of the microgrid and the application of fuzzification in the analysis are expounded upon in Sections 3, 4, respectively. Section 5 undertakes numerical investigations about the articulated model, while the conclusions derived from this study are deliberated upon in Section 6.

2 Microgrid: a brief overview

A microgrid denotes a diminutive power system or localized power station characterized by independent operational capacity or parallel connectivity with other small-scale power grids (Adefarati and Bansal, 2017; Adefarati et al., 2017; Wesly et al., 2020). The functioning of a microgrid system relies on communication infrastructure. It incorporates distributed generation technologies, including photovoltaic (PV) systems, wind turbine generation (WTG), diesel generators, and battery systems, as depicted in

TABLE 1 Probability of the wind subsystem being in different states.

State	Probability	State	Probability
1	0.99203	5	9.3×10^{-6}
2	0.002484	6	8.1×10^{-6}
3	0.0027314	7	5.4×10^{-6}
4	0.0027208	8	3.64×10^{-6}

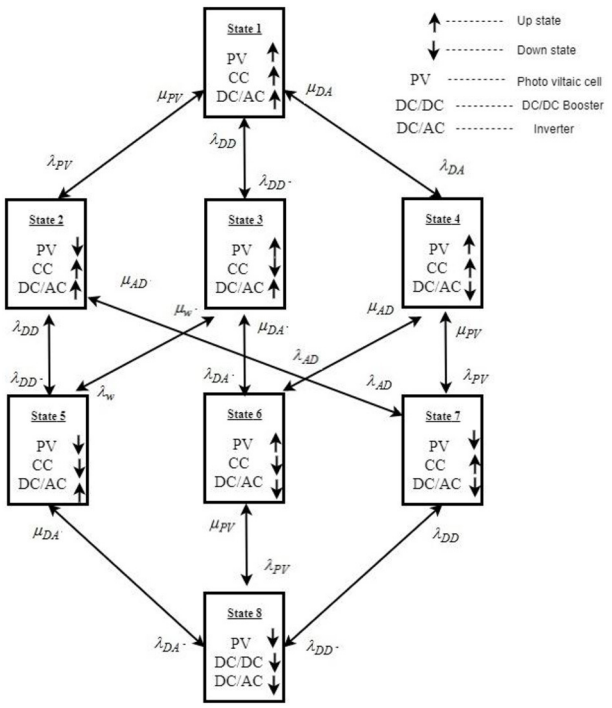

FIGURE 4
Eight-state Markov model of the PV subsystem.

Figure 1. The main goal of implementing microgrid systems over conventional power systems is to enhance local energy delivery, optimize energy efficiency, realize cost efficiencies, ameliorate grid safety through congestion reduction, generate utility revenue, bolster grid resilience, accrue savings on energy expenditures, stimulate economic growth in rural areas, diminish electricity costs, and ensure a reliable power supply. This approach concurrently contributes to lower greenhouse gas (GHG) emissions (Klir and Yuan, 1996; Kabir and Papadopoulos, 2018). The ensuing discussion succinctly outlines the principal components integral to the proposed microgrid.

2.1 Wind turbine generator

The power curve serves as a tool for assessing the generated power value by the WTG in relation to varying wind speeds (Tazvinga et al., 2017). The output of the WTG is contingent upon the wind speed at the hub height, geographical coordinates, and operational characteristics specific to the WTG (Del Granado et al., 2016).

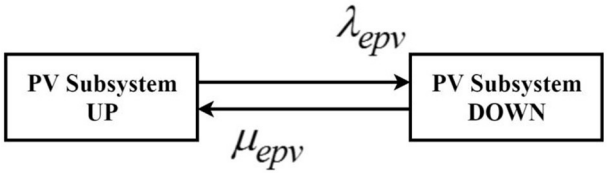

FIGURE 5
Equivalent two-state Markov model of PV subsystem.

TABLE 2 Probability of the PV subsystem being in different states.

State	Probability	State	Probability
1	0.994039	5	2.75×10^{-6}
2	0.002178	6	2.802×10^{-6}
3	0.00104	7	5.955×10^{-6}
4	0.002726	8	1.5×10^{-8}

2.2 Photovoltaic system

Solar energy undergoes direct conversion into electrical power through the application of photovoltaic (PV) panels, serving diverse functionalities within microgrid systems (Tazvinga et al., 2017). The PV system possesses the capability to be interconnected in both parallel and series configurations, strategically aligned to fulfill the instantaneous power requisites of consumers at a given time. The functionality of the PV system exhibits temporal variation due to fluctuations in solar irradiation conditions, temperature, geographical positioning, weather dynamics, and load patterns (Wu and Xia, 2015).

2.3 Battery energy storage system

The battery energy storage system (BESS) functions as an electrochemical apparatus designed to accumulate energy derived from diverse sources, such as photovoltaic (PV) and Wind Turbine Generator (WTG), offering versatility for multiple applications. Its integration into a microgrid system is imperative due to the inherently stochastic nature of solar and wind resources. The BESS is instrumental in addressing scenarios characterized by energy scarcity, ensuring the provision of stored energy to designated load points. Conversely, it is engineered to store surplus power generated by the microgrid system when the power output exceeds consumer demand. The operational dynamics of the BESS are evaluated through the assessment of its state of charge (SOC).

3 Reliability evaluation of microgrid

Every element depicted in Figure 1 possesses the capacity to exist in either an operational (UP) state or a non-operational (DOWN) state. When a subsystem lacks redundancy in its components, the failure of any individual element within the subsystem precipitates the failure of the entire subsystem. In

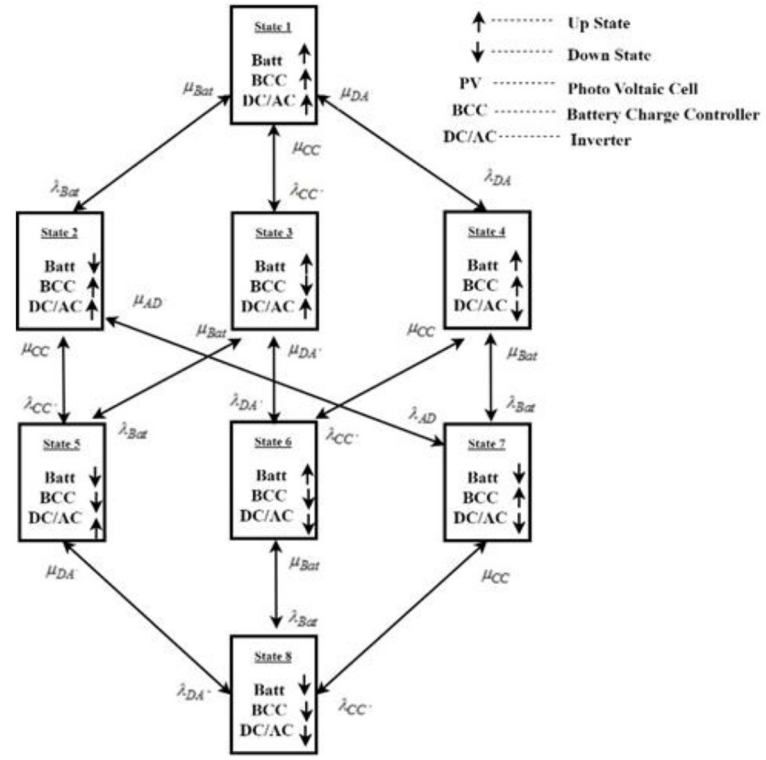

FIGURE 6
Eight-state Markov model of BES subsystem.

such instances, from a reliability perspective, the components of the subsystem are considered to be arranged in series. The subsequent subsections elucidate the state-space representation for each microgrid subsystem.

3.1 Wind turbine generator

The wind subsystem comprises a WTG, an AC-to-DC converter, and an inverter. Figure 2 depicts the 8-state Markov model of the wind subsystem. State 1 is the working state or UP state of the wind subsystem, and the remaining states are DOWN states caused by the failure of components of the wind subsystem. Combining states 2–8 in the Markov model, which leads to the wind subsystem failure, into a unified DOWN state, Figure 3 illustrates the resulting two-state Markov model for the wind subsystem. The parameters for this equivalent model are outlined below. The equivalent failure rate of the wind subsystem is shown in Equation 1.

$$\lambda_{ws} = \lambda_w + \lambda_{AD} + \lambda_{DA} \tag{1}$$

The equivalent repair rate of the wind subsystem is shown in Equation 2.

$$\mu_{ws} = (\lambda_w + \lambda_{AD} + \lambda_{DA}) \times \left(\frac{\lambda_w}{\mu_w} + \frac{\lambda_{AD}}{\mu_{AD}} + \frac{\lambda_{DA}}{\mu_{DA}}\right)^{-1} \tag{2}$$

The probability of being at the UP state and DOWN state in the wind subsystem equivalent model is given in Equations 3, 4, respectively.

$$Pup_{ws} = \left(1 + \frac{\lambda_w}{\mu_w} + \frac{\lambda_{AD}}{\mu_{AD}} + \frac{\lambda_{DA}}{\mu_{DA}}\right)^{-1} \tag{3}$$

$$Pdn_{ws} = \left(\frac{\lambda_w}{\mu_w} + \frac{\lambda_{AD}}{\mu_{AD}} + \frac{\lambda_{DA}}{\mu_{DA}}\right) \times \left(1 + \frac{\lambda_w}{\mu_w} + \frac{\lambda_{AD}}{\mu_{AD}} + \frac{\lambda_{DA}}{\mu_{DA}}\right)^{-1} \tag{4}$$

However, the probabilities of being in state 1, state 2, state 3, state 4, state 5, state 6, state 7, and state 8 can be derived from the 8-state Markov model as follows. The limiting probabilities corresponding to these states are P1, P2, P3, P4, P5, P6, P7, and P8.

$$\alpha P = \alpha \tag{5}$$

Here, α and P are limiting probability vectors and stochastic transitional probability matrices, respectively, as given in Equation 5.

$$[P1\ P2\ P3\ P4\ P5\ P6\ P7\ P8] \times P = [P1\ P2\ P3\ P4\ P5\ P6\ P7\ P8] \tag{6}$$

The stochastic transitional probability matrix is given in Equation 7. Putting the values of failure and repair rates of each component [19].

$$p = \begin{bmatrix} \mathbf{A_1} & \lambda_\omega & \lambda_{AD} & \lambda_{DA} & 0 & 0 & 0 & 0 \\ \mu_\omega & \mathbf{A_2} & 0 & 0 & \lambda_{AD} & 0 & \lambda_{DA} & 0 \\ \mu_{AD} & 0 & \mathbf{A_3} & 0 & \lambda_\omega & \lambda_{DA} & 0 & 0 \\ \mu_{DA} & 0 & 0 & \mathbf{A_4} & \mu_\omega & 0 & \mu_\omega & 0 \\ 0 & \mu_{AD} & \mu_\omega & 0 & \mathbf{A_5} & 0 & 0 & \lambda_{DA} \\ 0 & 0 & \mu_{DA} & \mu_{AD} & 0 & \mathbf{A_6} & 0 & \lambda_\omega \\ 0 & \mu_{DA} & 0 & \mu_\omega & 0 & 0 & \mathbf{A_7} & \lambda_{DD} \\ 0 & 0 & 0 & 0 & \mu_{DA} & \mu_\omega & \mu_{AD} & \mathbf{A_8} \end{bmatrix} \tag{7}$$

$$\begin{aligned} \mathbf{A_1} &= 1 - \lambda_\omega - \lambda_{AD} - \lambda_{DA} \\ \mathbf{A_2} &= 1 - \mu_\omega - \lambda_{AD} - \lambda_{DA} \\ \mathbf{A_3} &= 1 - \mu_{AD} - \lambda_\omega - \lambda_{DA} \\ \mathbf{A_4} &= 1 - \mu_{DA} - \lambda_\omega - \lambda_{DA} \\ \mathbf{A_5} &= 1 - \mu_{DA} - \mu_\omega - \lambda_{DA} \\ \mathbf{A_6} &= 1 - \mu_\omega - \mu_{DA} - \lambda_{AD} \\ \mathbf{A_7} &= 1 - \mu_\omega - \mu_{DA} - \lambda_{AD} \\ \mathbf{A_8} &= 1 - \mu_\omega - \mu_{AD} - \mu_{DA} \end{aligned}$$

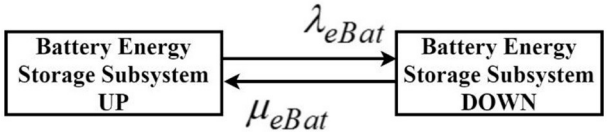

FIGURE 7
Equivalent two-state Markov model of BES subsystem.

TABLE 3 Probability of the BES subsystem being in different states.

State	Probability	State	Probability
1	0.994039	5	2.75×10^{-6}
2	0.002178	6	2.802×10^{-6}
3	0.00104	7	5.955×10^{-6}
4	0.002726	8	1.5×10^{-8}

$$p = \begin{bmatrix} .655 & .05 & .152 & .143 & 0 & 0 & 0 & 0 \\ 20 & -19.295 & 0 & 0 & .152 & 0 & .143 & 0 \\ 55.232 & 0 & -54.425 & 0 & .05 & .143 & 0 & 0 \\ 52.143 & 0 & 0 & -51.345 & 0 & 0 & 0.05 & 0 \\ 0 & 55.232 & 20 & 0 & -74.374 & 0 & 0 & .143 \\ 0 & 0 & 52.143 & 55.232 & 0 & -106.425 & 0 & .05 \\ 0 & 52.143 & 0 & 20 & 0 & 0 & -126.375 & 55.02 \\ 0 & 0 & 0 & 0 & 52.143 & 20 & 55.232 & -126.38 \end{bmatrix} \tag{8}$$

From Equations 6, 8

$$0.665P1 + 20P2 + 55.232P3 + 52.143P4 = P1 \tag{9a}$$
$$0.05P1 - 19.925P2 + 55.232P5 + 52.143P7 = P2 \tag{9b}$$
$$0.125P1 - 54.425P3 + 20P5 + 52.143P6 = P3 \tag{9c}$$
$$0.143P1 - 51.345P4 + 55.232P6 + 20P7 = P4 \tag{9d}$$
$$0.152P2 + 0.05P3 - 74.375P5 + 52.143P8 = P5 \tag{9e}$$
$$0.143P3 + 0.152P4 - 166.42P6 + 20P8 = P6 \tag{9f}$$

For any system, the summation of the probability of all the states is 1.

$$P1 + P2 + P3 + P4 + P5 + P6 + P7 + P8 = 1 \tag{10}$$

The probabilities of the wind subsystem being in different states can be obtained by solving Equations 9, 10, as shown in Table 1. The probability of the wind subsystem being in UP state is $P_{up} = P1 = 0.99203$. The probability of the wind subsystem being in a DOWN state is $P_{Down} = P2 + P3 + P4 + P5 + P6 + P7 + P8 = 0.00797$.

3.2 PV subsystem

The PV subsystem comprises PV cells, a DC-to-DC booster, and an inverter. Figure 4 depicts the 8-state Markov model of the PV subsystem. State 1 is the working state or UP state of the PV subsystem, and the remaining states are DOWN states caused by the failure of the PV subsystem's components. Combining states 2–8 in the Markov model, which leads to the failure of the PV subsystem, into a consolidated DOWN state, Figure 5 depicts the resulting two-state Markov model for the PV subsystem. The parameters for this equivalent model are detailed as follows.

The equivalent failure rate and repair rate are shown in Equations 11, 12, respectively.

$$\lambda_{pvs} = \lambda_{pv} + \lambda_{DD} + \lambda_{DA} \tag{11}$$
$$\mu_{pvs} = \left(\lambda_{pv} + \lambda_{DD} + \lambda_{DA}\right) \times \left(\frac{\lambda_{pv}}{\mu_{pv}} + \frac{\lambda_{DD}}{\mu_{DD}} + \frac{\lambda_{DA}}{\mu_{DA}}\right)^{-1} \tag{12}$$

The probability of being at the UP state and DOWN state in the PV subsystem equivalent model is given in Equations 13, 14, respectively.

$$Pup_{pv} = \left(1 + \frac{\lambda_{pv}}{\mu_{pv}} + \frac{\lambda_{DD}}{\mu_{DD}} + \frac{\lambda_{DA}}{\mu_{DA}}\right)^{-1} \tag{13}$$
$$Pdn_{pv} = \left(\frac{\lambda_{pv}}{\mu_{pv}} + \frac{\lambda_{DD}}{\mu_{DD}} + \frac{\lambda_{DA}}{\mu_{DA}}\right) \times \left(1 + \frac{\lambda_{pv}}{\mu_{pv}} + \frac{\lambda_{DD}}{\mu_{DD}} + \frac{\lambda_{DA}}{\mu_{DA}}\right)^{-1} \tag{14}$$

The stochastic transitional probability matrix in Equation 15 of the PV subsystem is computed by using the failure and repair rates

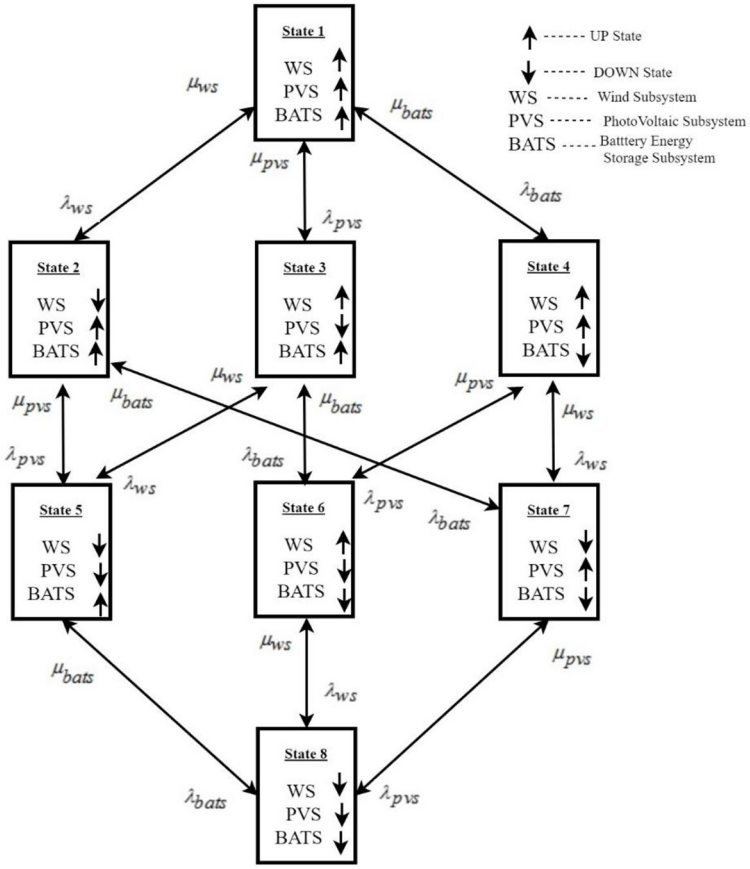

FIGURE 8
Markov model of microgrid.

TABLE 4 Probability of the microgrid being in different states.

State	Probability	State	Probability
1	0.98068	5	2.545×10^{-6}
2	0.0073175	6	3.2×10^{-6}
3	0.006014	7	5.716×10^{-6}
4	0.00597104	8	2.68×10^{-8}

TABLE 5 Equivalent parameters of wind subsystem.

	95%	Crisp value	105%
λ_{ew}	0.3021	0.318	0.3339
μ_{ew}	36.4164	42.3681	49.1693
Pup_{ws}	0.991773	0.99255	0.993255
Pdn_{ws}	0.00674501	0.00744972	0.00822745

of each component (Adefarati and Bansal, 2017).

$$p = \begin{bmatrix} \mathbf{B_1} & \lambda_{pv} & \lambda_{DD} & \lambda_{DA} & 0 & 0 & 0 & 0 \\ \mu_{pv} & \mathbf{B_2} & 0 & 0 & \lambda_{DD} & 0 & \lambda_{DA} & 0 \\ \mu_{DD} & 0 & \mathbf{B_3} & 0 & \lambda_{pv} & \lambda_{DA} & 0 & 0 \\ \mu_{DA} & 0 & 0 & \mathbf{B_4} & \mu_{pv} & 0 & \mu_{pv} & 0 \\ 0 & \mu_{DD} & \mu_{pv} & 0 & \mathbf{B_5} & 0 & 0 & \lambda_{DA} \\ 0 & 0 & \mu_{DA} & \mu_{DD} & 0 & \mathbf{B_6} & 0 & \lambda_{pv} \\ 0 & \mu_{DA} & 0 & \mu_{pv} & 0 & 0 & \mathbf{B_7} & \lambda_{DD} \\ 0 & 0 & 0 & 0 & \mu_{DA} & \mu_{pv} & \mu_{DD} & \mathbf{B_8} \end{bmatrix} \quad (15)$$

$$\mathbf{B_1} = 1 - \lambda_{pv} - \lambda_{DD} - \lambda_{DA}$$
$$\mathbf{B_2} = 1 - \mu_{pv} - \lambda_{DD} - \lambda_{DA}$$
$$\mathbf{B_3} = 1 - \mu_{DD} - \lambda_{pv} - \lambda_{DA}$$
$$\mathbf{B_4} = 1 - \mu_{DA} - \lambda_{\omega} - \lambda_{DA}$$
$$\mathbf{B_5} = 1 - \mu_{DA} - \mu_{pv} - \lambda_{DA}$$
$$\mathbf{B_6} = 1 - \mu_{pv} - \mu_{DA} - \lambda_{DD}$$
$$\mathbf{B_7} = 1 - \mu_{pv} - \mu_{DA} - \lambda_{DD}$$
$$\mathbf{B_8} = 1 - \mu_{pv} - \mu_{DD} - \mu_{DA}$$

However, the probability of being in state 1, state 2, state 3, state 4, state 5, state 6, state 7, and state 8 can be derived from the 8-state Markov model of the PV subsystem using Equations 5, 6, 15. The limiting probabilities corresponding to these states are P1, P2, P3, P4, P5, P6, P7, and P8. Table 2 shows the probabilities of PV subsystems in different systems.

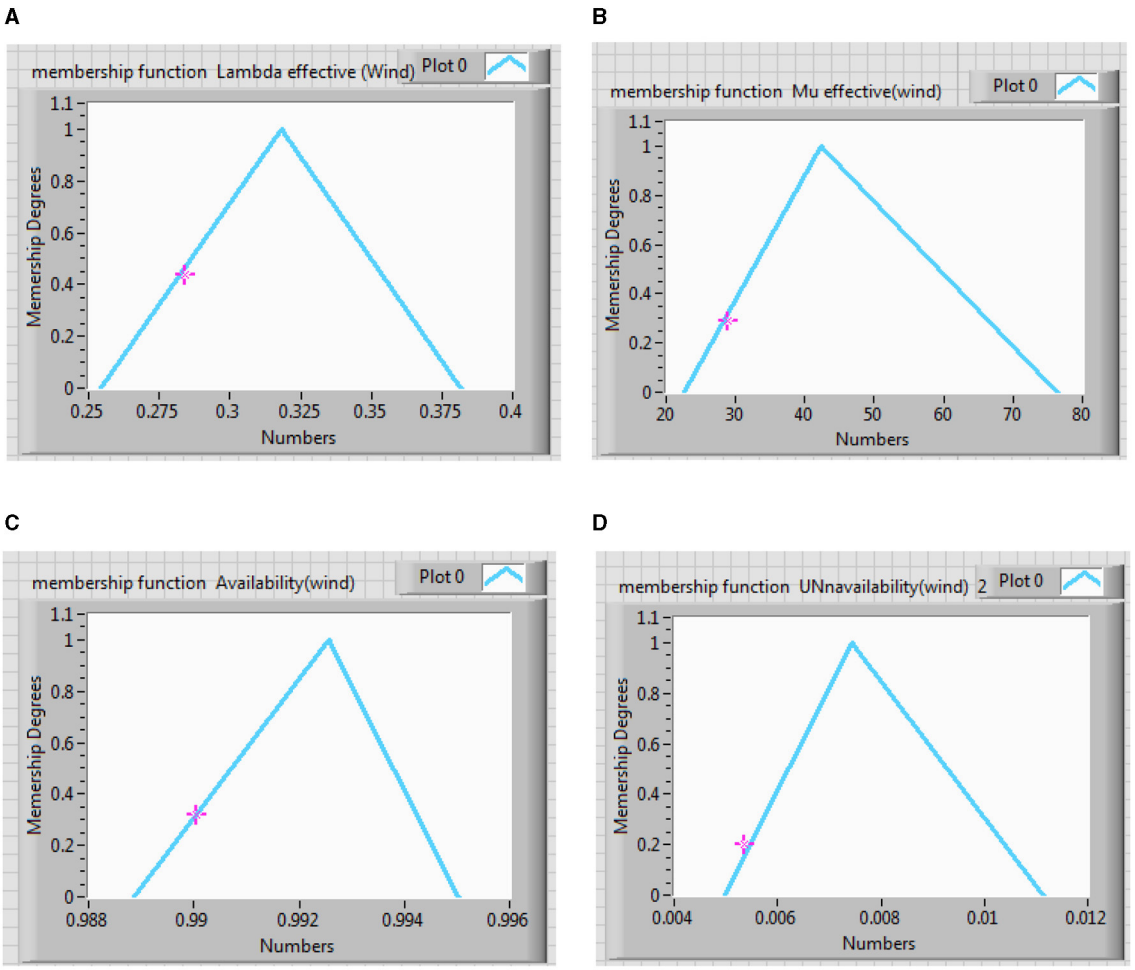

FIGURE 9
Membership function effective, **(A)** failure rate of wind subsystem, **(B)** repair rate of wind subsystem, **(C)** availability of wind subsystem, and **(D)** unavailability of wind subsystem.

3.3 Battery energy storage subsystem

The battery energy storage subsystem comprises a battery bank, battery charge controller, and inverter. Figure 6 depicts the 8-state Markov model of the BES subsystem. State 1 is the working state or UP state of the BES subsystem, and the remaining states are DOWN states caused by the failure of components of the BES subsystem.

The consolidation of states 2–8 in the Markov model is undertaken due to the resultant failure of the BES subsystem. These states are amalgamated into a unified DOWN state, as illustrated in Figure 7, representing the equivalent two-state Markov model for the BES subsystem. The parameters delineating this equivalent model are provided as follows. The equivalent failure rate and repair rate are shown in Equations 16, 17, respectively.

$$\lambda_{bats} = \lambda_{Bat} + \lambda_{CC} + \lambda_{DA} \tag{16}$$

$$\mu_{bats} = (\lambda_{Bat} + \lambda_{cc} + \lambda_{DA}) \times \left(\frac{\lambda_{Bat}}{\mu_{Bat}} + \frac{\lambda_{cc}}{\mu cc} + \frac{\lambda_{DA}}{\mu_{DA}}\right)^{-1} \tag{17}$$

$$Pup_{bat} = \left(1 + \frac{\lambda_{Bat}}{\mu_{Bat}} + \frac{\lambda_{cc}}{\mu_{cc}} + \frac{\lambda_{DA}}{\mu_{DA}}\right)^{-1} \tag{18}$$

$$Pdn_{bat} = \left(\frac{\lambda_{Bat}}{\mu_{Bat}} + \frac{\lambda_{cc}}{\mu cc} + \frac{\lambda_{DA}}{\mu_{DA}}\right) + \left(1 + \frac{\lambda_{Bat}}{\mu_{Bat}} + \frac{\lambda_{cc}}{\mu_{cc}} + \frac{\lambda_{DA}}{\mu_{DA}}\right)^{-1} \tag{19}$$

The probability of being at the UP state and DOWN state in the BES subsystem equivalent model is given in Equations 18, 19, respectively.

However, the probability of being in state 1, state 2, state 3, state 4, state 5, state 6, state 7, and state 8 can be derived from the 8-state Markov model of the BES subsystem using Equations 5, 6, 15. The limiting probabilities corresponding to these states are P1, P2, P3, P4, P5, P6, P7, and P8. The stochastic transitional probability matrix of BES is given in Equation 20.

$$p = \begin{bmatrix} \mathbf{E_1} & \lambda_{Bat} & \lambda_{CC} & \lambda_{DA} & 0 & 0 & 0 & 0 \\ \mu_{Bat} & \mathbf{E_2} & 0 & 0 & \lambda_{CC} & 0 & \lambda_{DA} & 0 \\ \mu_{CC} & 0 & \mathbf{E_3} & 0 & \lambda_{Bat} & \lambda_{DA} & 0 & 0 \\ \mu_{DA} & 0 & 0 & \mathbf{E_4} & \mu_{Bat} & 0 & \mu_{Bat} & 0 \\ 0 & \mu_{CC} & \mu_{Bat} & 0 & \mathbf{E_5} & 0 & 0 & \lambda_{DA} \\ 0 & 0 & \mu_{DA} & \mu_{CC} & 0 & \mathbf{E_6} & 0 & \lambda_{Bat} \\ 0 & \mu_{DA} & 0 & \mu_{Bat} & 0 & 0 & \mathbf{E_7} & \lambda_{CC} \\ 0 & 0 & 0 & 0 & \mu_{DA} & \mu_{Bat} & \mu_{CC} & \mathbf{E_8} \end{bmatrix} \tag{20}$$

TABLE 6 Effective failure rate, repair rate, availability, and unavailability of wind subsystem.

α	λ_{ew1}	λ_{ew2}	μ_{ew1}	μ_{ew2}	Pup_{ws1}	Pup_{ws2}	Pdn_{ws1}	Pdn_{ws2}
0	0.30231	0.334224	36.4164	49.1693	0.991773	0.993255	0.00674501	0.00822745
0.1	0.303899	0.332347	37.0108	48.5343	0.991854	0.993182	0.00682491	0.00815343
0.2	0.305632	0.331047	37.6173	47.8267	0.991933	0.99311	0.00688989	0.00807401
0.3	0.307076	0.329314	38.3249	47.0686	0.992005	0.993038	0.00696209	0.00799458
0.4	0.308375	0.327726	38.8303	46.4621	0.992099	0.992966	0.00702708	0.00792238
0.5	0.310108	0.325993	39.4874	45.7545	0.992164	0.992901	0.00709928	0.00784296
0.6	0.311841	0.324404	39.9928	45.0975	0.992236	0.992829	0.00717148	0.00775632
0.7	0.313285	0.32296	40.4982	44.4404	0.992316	0.992764	0.00723646	0.00769856
0.8	0.314874	0.321227	41.1552	43.7834	0.992388	0.992691	0.00731588	0.00760469
0.9	0.316318	0.319928	41.8123	43.0758	0.99246	0.992619	0.00738087	0.00753971
1.0	0.318195	0.318195	42.4188	42.4188	0.99255	0.99255	0.00744972	0.00744972

TABLE 7 Equivalent parameters of wind subsystem.

	95%	Crisp value	105%
λ_{epv}	0.236265	0.2487	0.261135
μ_{epv}	35.7139	41.5508	48.2208
Pup_{pv}	0.993428	0.99405	0.994614
Pdn_{pv}	0.00538623	0.00594983	0.00657201

$$\begin{aligned}
\mathbf{E_1} &= 1 - \lambda_{Bat} - \lambda_{CC} - \lambda_{DA} \\
\mathbf{E_2} &= 1 - \mu_{Bat} - \lambda_{CC} - \lambda_{DA} \\
\mathbf{E_3} &= 1 - \mu_{CC} - \lambda_{Bat} - \lambda_{DA} \\
\mathbf{E_4} &= 1 - \mu_{DA} - \lambda_{Bat} - \lambda_{DA} \\
\mathbf{E_5} &= 1 - \mu_{DA} - \mu_{Bat} - \lambda_{DA} \\
\mathbf{E_6} &= 1 - \mu_{Bat} - \mu_{DA} - \lambda_{CC} \\
\mathbf{E_7} &= 1 - \mu_{Bat} - \mu_{DA} - \lambda_{CC} \\
\mathbf{E_8} &= 1 - \mu_{Bat} - \mu_{CC} - \mu_{DA}
\end{aligned}$$

The probability of the BES subsystem being in the UP state is $P_{up} = P1 = 0.99405$. The probability of the BES subsystem being in the DOWN state is $P_{Down} = P2+P3+P4+P5+P6+P7+P8 = 0.00594983$. Table 3 shows the probabilities of the BES subsystem.

3.4 Microgrid

Each component in Figure 8 can reside in either the UP state or DOWN state. It comprises three subsystems, i.e., the wind subsystem, the PV subsystem, and the battery energy storage subsystem, which are said to be in parallel from the reliability point of view. The equivalent parameters of this model are as follows (Billinton and Allan, 1992). Figure 8 shows the 8-state Markov model of microgrid. State 1 to state 7 are UP states and state 8 is the DOWN state. The equivalent repair rate

$$\mu_{mgd} = \mu_{ws} + \mu_{pvs} + \mu_{bats} \tag{21}$$

The equivalent failure rate

$$\lambda_{mgd} = \lambda_{ws} \times \lambda_{pvs} \times \lambda_{bats} \left(r_{ws}r_{pvs} + r_{pvs}r_{bats} + r_{bats}r_{ws}\right) \tag{22}$$

The availability,

$$Pup_{mgd} = \lambda_{ws} \times \lambda_{pvs} \times \lambda_{bats} \times r_{ws} \times r_{pvs} \times r_{bats} \tag{23}$$

Where, $r_{ws} = \frac{1}{\mu_{ws}}$, $r_{pvs} = \frac{1}{\mu_{pvs}}$, and $r_{bats} = \frac{1}{\mu_{bats}}$ are the probabilities of being in state 1, state 2, state 3, state 4, state 5, state 6, state 7, and state 8 can be derived from the 8-state Markov model of the microgrid using Equation 5 and stochastic transitional probability matrix of the microgrid given in Equation 24.

$$p = \begin{bmatrix}
F_1 & \lambda_{\omega s} & \lambda_{pvs} & \lambda_{bats} & 0 & 0 & 0 & 0 \\
\mu_{\omega s} & F_2 & 0 & 0 & \lambda_{pvs} & 0 & \lambda_{bats} & 0 \\
\mu_{pvs} & 0 & F_3 & 0 & \lambda_{ws} & \lambda_{bats} & 0 & 0 \\
\mu_{bats} & 0 & 0 & F_4 & \mu_{\omega s} & 0 & \mu_{\omega s} & 0 \\
0 & \mu_{pvs} & \mu_{\omega s} & 0 & F_5 & 0 & 0 & \lambda_{bats} \\
0 & 0 & \mu_{bats} & \mu_{pvs} & 0 & F_6 & 0 & \lambda_{\omega s} \\
0 & \mu_{bats} & 0 & \mu_{\omega s} & 0 & 0 & F_7 & \lambda_{pvs} \\
0 & 0 & 0 & 0 & \mu_{bats} & \mu_{ws} & \mu_{pvs} & F_8
\end{bmatrix} \tag{24}$$

$$\begin{aligned}
\mathbf{F_1} &= 1 - \lambda_{\omega s} - \lambda_{pvs} - \lambda_{bats} \\
\mathbf{F_2} &= 1 - \mu_{\omega s} - \lambda_{pvs} - \lambda_{bats} \\
\mathbf{F_3} &= 1 - \mu_{pvs} - \lambda_{\omega s} - \lambda_{bats} \\
\mathbf{F_4} &= 1 - \mu_{bats} - \lambda_{\omega s} - \lambda_{bats} \\
\mathbf{F_5} &= 1 - \mu_{bats} - \mu_{\omega s} - \lambda_{bats} \\
\mathbf{F_6} &= 1 - \mu_{\omega s} - \mu_{bats} - \lambda_{pvs} \\
\mathbf{F_7} &= 1 - \mu_{\omega s} - \mu_{bats} - \lambda_{pvs} \\
\mathbf{F_8} &= 1 - \mu_{\omega s} - \mu_{pvs} - \mu_{bats}
\end{aligned}$$

The limiting probabilities corresponding to these states are P1, P2, P3, P4, P5, P6, P7, and P8. The stochastic transitional probability matrix in Equation 24 of the microgrid is computed by using the equivalent failure rates and equivalent repair rates of each subsystem. Since the subsystems are in parallel, the availability of

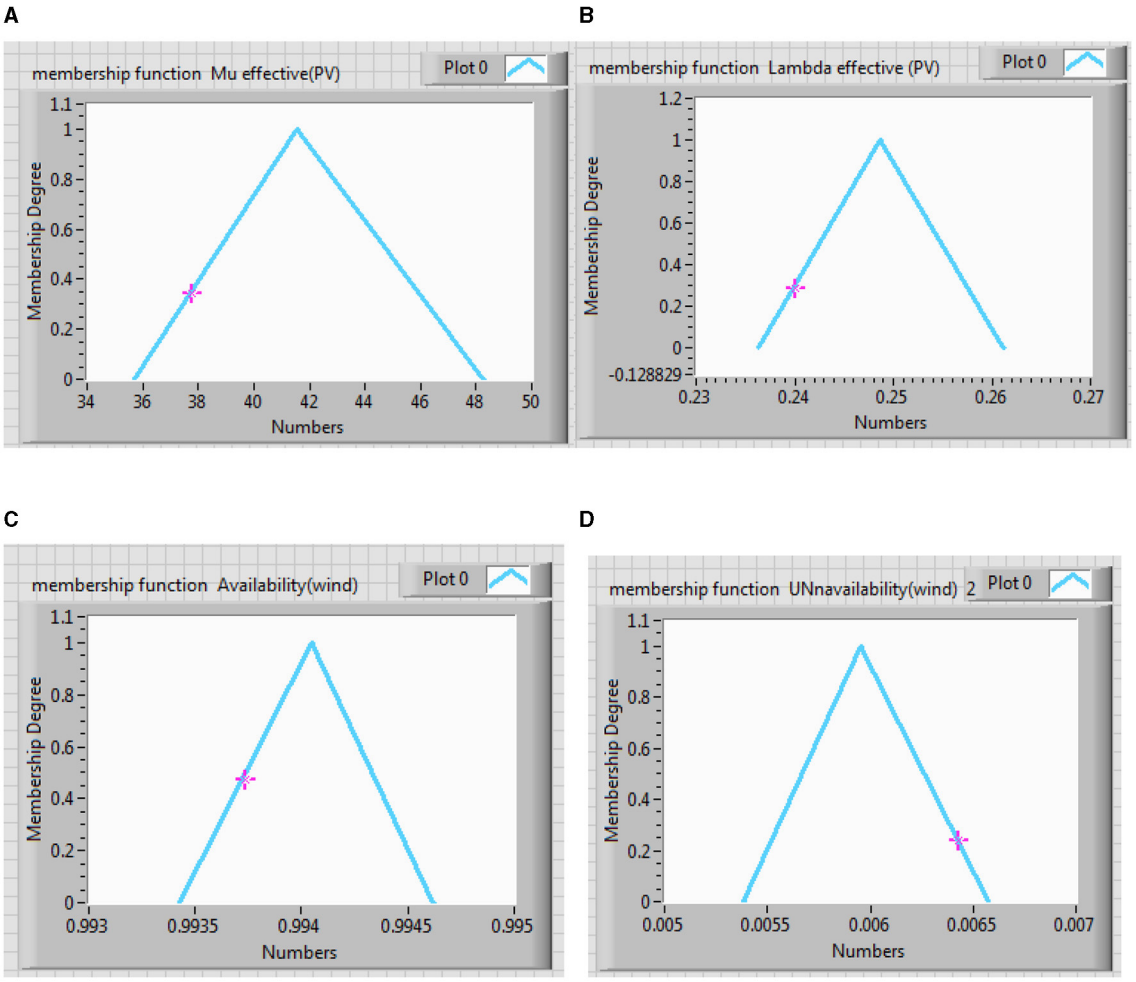

FIGURE 10
Membership function effective **(A)** failure rate, **(B)** repair rate, **(C)** availability, and **(D)** unavailability of PV subsystem.

the microgrid system, the summation of the probability of all the states as given in Equation 10, is 1. From Equations 5, 21,

$$0.1341P1 + 42.3681P2 + 41.5508P3 + 48.9878P4 = P1 \quad (25a)$$
$$0.318P1 - 41.916P2 + 41.5508P5 + 48.9878P7 = P2 \quad (25b)$$
$$0.2487P1 - 41.168P3 + 42.3681P5 + 48.9878P6 = P3 \quad (25c)$$
$$0.2992P1 - 48.5357P4 + 41.5508P6 + 48.3681P7 = P4 \quad (25d)$$
$$0.2487P2 + 0.318P3 - 83.2181P5 + 48.98P8 = P5 \quad (25e)$$
$$0.2992P3 + 0.2487P4 - 89.8566P6 + 42.3681P8 = P6 \quad (25f)$$
$$0.2992P2 + 0.318P4 - 90.6046P7 + 41.5508P8 = P7 \quad (25g)$$
$$\mathbf{0.2992P5 + 0.318P6 + 0.2487P - 131.9007P8 = P8} \quad (25h)$$

By solving the linear Equations 10, 25, the probability of the microgrid being in different states is given in Table 4. Since the subsystems are in parallel with the availability of the microgrid system, the probability of the microgrid being in UP state is Pup_{mgd} =P1+P2+P3+P4+P5+P6+P7 = 0.9999999989.

The probability of the BES subsystem being in the UP state is Pdn_{mgd} = P8 = 2.68 × 10-8. The probability of the microgrid to be in the UP state is

$$Pup_{mgd} = P1 + P2 + P3 + P4 + P5 + P6 + P7 = 0.9999999989.$$

The probability of the BES subsystem being in the UP state Pdn_{mgd} = P8 = 2.68 × 10-8.

4 Fuzzy Markov model-based reliability analysis

Fuzzy sets have been employed to account for inherent uncertainties in parameters, specifically failure and repair rates, during reliability calculations. Consequently, reliability parameters are represented as fuzzy numbers (Klir and Yuan, 1996; Zimmermann, 2011). The degree of uncertainty increases with the breadth of support of the membership function (Li and Yen, 1995). Computational efficiency is a critical concern in fuzzy analyses. Anzilli and Facchinetti (2019) demonstrated that computational complexity in fuzzy analyses can be mitigated by consolidating membership functions into alpha-cuts and

TABLE 8 Effective failure rate, repair rate, availability, and unavailability of PV subsystem.

α	λ_{epv1}	λ_{epv2}	μ_{epv1}	μ_{epv2}	Pup_{pv1}	Pup_{pv2}	Pdn_{pv1}	Pdn_{pv2}
0	0.236316	0.260827	35.8073	48.1927	0.993428	0.994614	0.00538623	0.00657201
0.1	0.237519	0.259925	36.2857	47.608	0.993491	0.994567	0.00544043	0.00652347
0.2	0.238872	0.258571	36.9236	46.9701	0.993549	0.994509	0.00550542	0.0064657
0.3	0.240075	0.257519	37.5083	46.2791	0.993614	0.994451	0.00555596	0.0063935
0.4	0.241278	0.256316	38.0399	45.6944	0.993671	0.994394	0.00562094	0.00633574
0.5	0.242481	0.254962	38.5714	44.897	0.993736	0.994329	0.00566426	0.00627076
0.6	0.243534	0.253609	39.2625	44.206	0.993801	0.994285	0.0057148	0.00620578
0.7	0.244887	0.252556	39.794	43.5681	0.993866	0.99422	0.005787	0.00614079
0.8	0.24609	0.251203	40.4319	43.0365	0.993924	0.99417	0.00584477	0.00608303
0.9	0.247293	0.25015	41.0166	42.2924	0.993982	0.994112	0.00590253	0.00601083
1.0	0.248797	0.248797	41.5482	41.5482	0.99405	0.99405	0.00594983	0.00594983

TABLE 9 Equivalent parameters of the BES subsystem.

	95%	Crisp value	105%
λ_{eBat}	0.28424	0.2992	0.31416
μ_{eBat}	42.1062	48.9878	56.8516
Pup_{bat}	0.993295	0.993929	0.994504
Pdn_{bat}	0.0054956	0.00607057	0.00670529

performing mathematical operations within these intervals. The crisp set comprising elements belonging to a fuzzy set to at least the degree alpha is termed the α-cut of that fuzzy set. The ensuing procedural steps delineate the application of fuzzy reliability analysis to the microgrid.

Steps of Procedure:

Step 1: Express the input data, specifically failure and repair rates, through the utilization of fuzzy numbers. Determine membership functions based on past data or expert input.
Step 2: Establish alpha cuts of input data for $\alpha \in [0,1]$.
Step 3: Determine the parameters of the equivalent reliability model for any specified α by employing the set of Equations 21–23 and utilizing fuzzy arithmetic operations. For each α-cut of the fuzzy number representing a parameter, perform calculations based on Equations 21–23 to ascertain the minimum and maximum attainable values of the output.
Step 4: The results computed in Step 3 are employed to formulate fuzzy outputs.

5 Case study and discussion

This section showcases specific investigations aimed at illustrating the advantages inherent in the proposed reliability model. The preceding Section 3, scrutinized the crisp model, whereas the focus here lies on the examination of fuzzy models. In the realm of reliability studies, it is observed that reliability transition rates exhibit asymmetry and are characterized by single-kernel fuzzy numbers.

5.1 Wind subsystem

Table 5 presents the equivalent failure rate, repair rate, availability, and unavailability fuzzy values considering 5% of crisp value. Figure 9 depicts the membership function of effective failure rate, repair rate, availability, and unavailability of wind subsystem at different cuts from 0 to 1. The fuzzy calculation is employed to analyze the equivalent two-state model. Table 6 presents the 11 cuts for these parameters.

Comparing Tables 5, 6, it can be observed that fuzzy results with alpha equal to 1 are expectedly identical to crisp results. In Figures 9A, D are approximately symmetrical, while Figures 9B, C are unsymmetrical. The Center of Area (CA) of Figures 9B, C are not equal to their kernels, which is caused by the uncertainties in the input data. The results of fuzzy analyses are more realistic than those of crisp study. In addition, the triangular membership function has been used because its results incorporate the effect of uncertainties appropriately, and its corresponding computations are plain.

5.2 PV subsystem

Table 7 presents the equivalent failure rate, repair rate, availability, and unavailability fuzzy values considering 5% of crisp value. Figure 10 depicts the membership function of effective failure rate, repair rate, availability, and unavailability of PV subsystem at different alpha cuts from 0 to 1. Table 8 shows 11 cuts for these parameters.

Comparing Tables 7, 8, it can be observed that fuzzy results with alpha equal to 1 are expectedly identical to crisp results. In Figures 10A, D are approximately symmetrical, while Figures 10B, C are unsymmetrical. The Center of Area (CA) of Figures 10B, C are not equal to their kernels, which is caused by the uncertainties

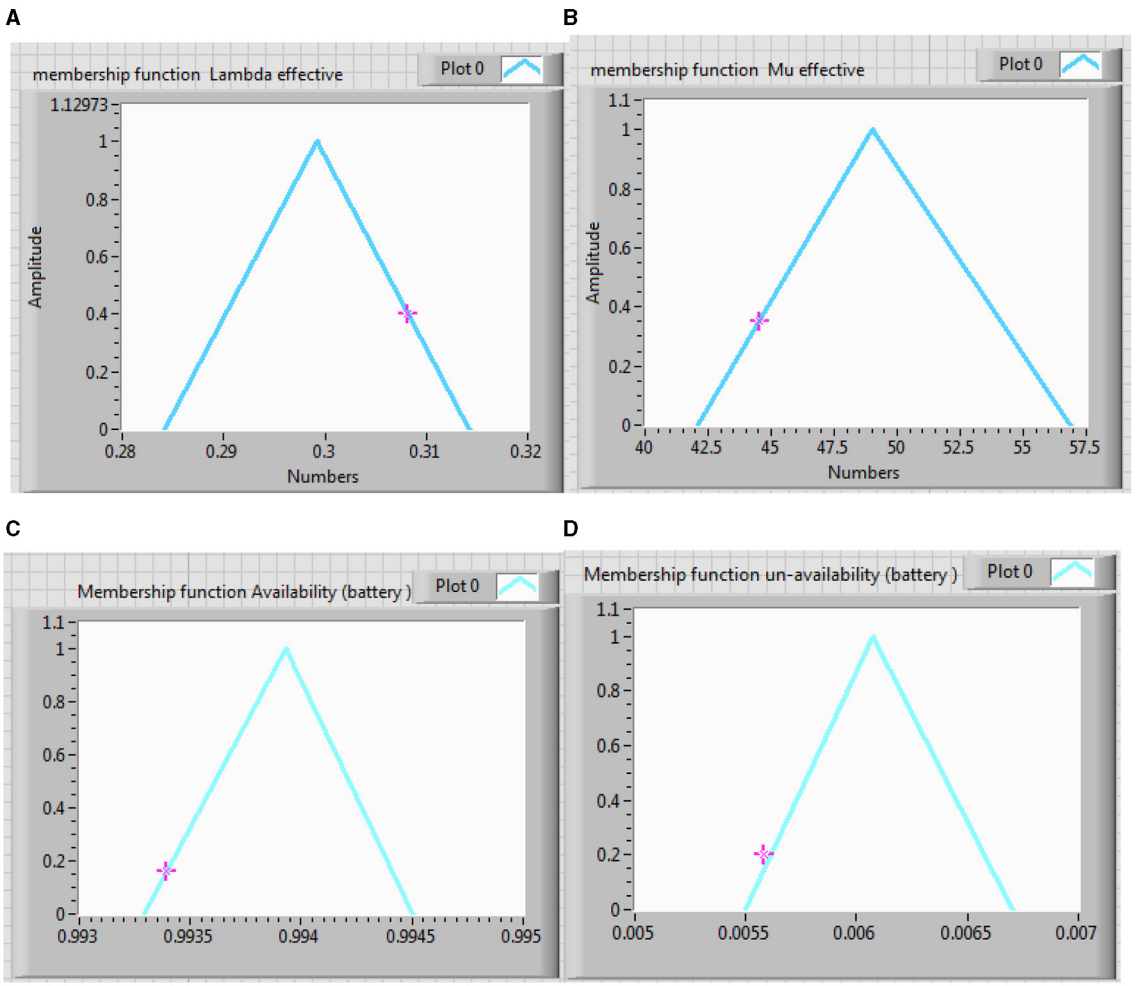

FIGURE 11
Membership function effective **(A)** failure rate, **(B)** repair rate, **(C)** availability, and **(D)** unavailability of battery energy storage system.

TABLE 10 **Effective failure rate, repair rate, availability, and unavailability of BES subsystem.**

α	λ_{eBat1}	λ_{eBat2}	μ_{eBat1}	μ_{eBat2}	Pup_{Bat1}	Pup_{Bat2}	Pdn_{Bat1}	Pdn_{Bat2}
0	0.28424	0.314801	42.1062	56.8516	0.993295	0.994504	0.0054956	0.00670529
0.1	0.285736	0.31278	42.8488	56.1628	0.993383	0.994437	0.006617	0.005563
0.2	0.287245	0.311191	43.5465	55.3488	0.993426	0.994394	0.006574	0.005606
0.3	0.288906	0.309747	44.1279	54.4767	0.993491	0.994336	0.006509	0.005664
0.4	0.290113	0.308303	44.8837	53.7791	0.993556	0.994271	0.006444	0.005729
0.5	0.291774	0.306859	45.5814	52.9651	0.993621	0.994213	0.006379	0.005787
0.6	0.293132	0.305271	46.2791	52.1512	0.993671	0.994162	0.006329	0.005838
0.7	0.294792	0.303971	46.9767	51.4535	0.993751	0.994119	0.006249	0.005881
0.8	0.296151	0.302238	47.6744	50.6395	0.993809	0.994061	0.006191	0.005939
0.9	0.297811	0.30065	48.314	49.8837	0.993866	0.993996	0.006134	0.006004
1.0	0.299321	0.299321	48.9878	48.9878	0.993929	0.993929	0.00607057	0.00607057

TABLE 11 Equivalent parameters of microgrid subsystem.

	95%	Crisp value	105%
λ_{ews}	0.3021	0.318	0.3339
λ_{epvs}	0.236265	0.2487	0.261135
λ_{ebs}	0.28424	0.2992	0.31416
μ_{ews}	40.2497	42.3681	44.4865
μ_{epvs}	39.4733	41.5508	43.6283
μ_{ebs}	46.5384	48.9878	51.4372

TABLE 12 Effective failure rate, repair rate, availability, and unavailability of microgrid subsystem.

	95%	Crisp value	105%
λ_{emgd}	3.8535E-5	0.0000367	3.4865E-5
μ_{emgd}	126.261	132.9067	139.552
Pup_{emgd}	0.9499997381405364	0.9999997243 58459463849798	1.0499997 1057638
Pdn_{emgd}	2.618594635 093427E-7	0.00000027564 1540536150201	2.8942361 7562958E-7

in the input data. The results of fuzzy analyses are more realistic than those of crisp study. In addition, the triangular membership function has been used because its results incorporate the effect of uncertainties appropriately, and its corresponding computations are also plain.

5.3 Battery energy storage system

Table 9 presents the equivalent failure rate, repair rate, availability, and unavailability fuzzy values considering 5% of crisp value. Figure 11 depicts the membership function of effective failure rate, repair rate, availability, and unavailability of battery energy storage system at different alpha cuts from 0 to 1. Table 10 shows the 11 cuts for these parameters.

Comparing Tables 9, 10, it can be observed that fuzzy results with alpha equal to 1 are expectedly identical to crisp results. In Figures 11A, D are approximately symmetrical, while in Figures 11B, C are unsymmetrical. Center of Area (CA) of Figures 11B, C are not equal to their kernels, which is caused by the uncertainties in the input data. The results of fuzzy analyses are more realistic than those of crisp study. In addition, the triangular membership function has been used because its results incorporate the effect of uncertainties appropriately, and its corresponding computations are also plain.

5.4 Microgrid system

The equivalent failure rate repair, rate, availability, and unavailability of the microgrid are evaluated using Equations 21–23 and given in Tables 11, 12.

6 Conclusion

This study focuses on the reliability modeling of a microgrid, employing the Markov process approach. To address uncertainties in input parameters, fuzzy analysis is implemented, incorporating the effective alpha-cut method for precise calculations. The equivalent two-state model is applied to compute probabilities and transition rates within the microgrid reliability framework. A comparative analysis is conducted using a numerical example involving both crisp and fuzzy data. The findings indicate that assuming crisp parameters equal to the kernel of fuzzy parameters results in a lower microgrid availability when employing fuzzy calculations compared to crisp analysis. This discrepancy is ascribed to the inherent uncertainties present in the input data. The availability of the wind subsystem, PV subsystem, and battery subsystem are 0.99255, 0.99405, and 0.99392, respectively, at an alpha-cut =1. The overall availability of hybrid microgrids is 0.99999.

Data availability statement

The original contributions presented in the study are included in the article/supplementary material, further inquiries can be directed to the corresponding authors.

Author contributions

KS: Formal analysis, Writing – original draft, Writing – review & editing. MC: Writing – original draft, Writing – review & editing. IS: Data curation, Investigation, Writing – original draft, Writing – review & editing. APat: Conceptualization, Investigation, Writing – original draft, Writing – review & editing. JG: Conceptualization, Data curation, Investigation, Methodology, Visualization, Writing – original draft, Writing – review & editing. APan: Conceptualization, Investigation, Writing – original draft, Writing – review & editing. HQ: Conceptualization, Data curation, Methodology, Software, Writing – original draft, Writing – review & editing. SM: Conceptualization, Investigation, Software, Writing – original draft, Writing – review & editing.

Funding

The author(s) declare financial support was received for the research, authorship, and/or publication of this article. HQ thanks the USA NSF award 1663105, 1761839, and 2200138, a catalyst award from the USA National Academy of Medicine, AI Tennessee Initiative, and the support at the University of Tennessee at Chattanooga.

Conflict of interest

The authors declare that the research was conducted in the absence of any commercial or financial relationships that could be construed as a potential conflict of interest.

The author(s) declared that they were an editorial board member of Frontiers, at the time of submission. This had no impact on the peer review process and the final decision.

Publisher's note

References

Adefarati, T., and Bansal, R. C. (2017). Reliability and economic assessment of a microgrid power system with the integration of renewable energy resources. *Appl. Energy* 206, 911–933. doi: 10.1016/j.apenergy.2017.08.228

Adefarati, T., and Bansal, R. C. (2019). Reliability, economic and environmental analysis of a microgrid system in the presence of renewable energy resources. *Appl. Energy* 236, 1089–1114. doi: 10.1016/j.apenergy.2018.12.050

Adefarati, T., Bansal, R. C., and John Justo, J. (2017). Techno-economic analysis of a PV–wind–battery–diesel standalone power system in a remote area. *J. Eng.* 2017, 740–744. doi: 10.1049/joe.2017.0429

Ahshan, R., Iqbal, M. T., Mann, G. K., and Quaicoe, J. E. (2017). Microgrid reliability evaluation considering the intermittency effect of renewable energy sources. *Int. J. Smart Grid Clean Energy* 6, 252–268. doi: 10.12720/sgce.6.4.252-268

Akbari, M. G., and Hesamian, G. (2020). Time-dependent intuitionistic fuzzy system reliability analysis. *Soft Comput.* 24, 14441–14448. doi: 10.1007/s00500-020-04796-w

Ansari, O. A., Safari, N., and Chung, C. Y. (2016). "Reliability assessment of microgrid with renewable generation and prioritized loads," in *2016 IEEE Green Energy and Systems Conference (IGSEC)* (IEEE), 1–6. doi: 10.1109/IGESC.2016.7790067

Anzilli, L., and Facchinetti, G. (2019). "An alpha-cut evaluation of interval-valued fuzzy sets for application in decision making," in *Fuzzy Logic and Applications: 12th International Workshop, WILF 2018 Genoa, Italy, September 6–7, 2018* (Cham: Springer International Publishing), 193–211. doi: 10.1007/978-3-030-12544-8_16

Ashraf, S., Saleem, S., Ahmed, T., Aslam, Z., and Shuaeeb, M. (2020). "Iris and foot based sustainable biometric identification approach," in *2020 International Conference on Software, Telecommunications and Computer Networks (SoftCOM)* (IEEE), 1–6. doi: 10.23919/SoftCOM50211.2020.9238333

Billinton, R., and Allan, R. N. (1992). *Reliability Evaluation Of Engineering Systems*. New York: Plenum press. doi: 10.1007/978-1-4899-0685-4

Bowles, J. B., and Pelaez, C. E. (1995). Application of fuzzy logic to reliability engineering. *Proc. IEEE* 83, 435–449. doi: 10.1109/5.364489

Del Granado, P. C., Pang, Z., and Wallace, S. W. (2016). Synergy of smart grids and hybrid distributed generation on the value of energy storage. *Appl. Energy* 170, 476–488. doi: 10.1016/j.apenergy.2016.01.095

Kabir, S., and Papadopoulos, Y. (2018). A review of applications of fuzzy sets to safety and reliability engineering. *Int. J. Approx. Reason.* 100, 29–55. doi: 10.1016/j.ijar.2018.05.005

Khalili, T., Habibi, S. I., Abadi, S. A. G. K., Ahmadi, S., and Bidram, A. (2022). "Upside risk effect on reliability of microgrids considering demand response program and COVID-19: an investigation on health system and power system interactions," in *2022 IEEE Kansas Power and Energy Conference (KPEC)* (IEEE), 1–6. doi: 10.1109/KPEC54747.2022.9814788

Khare, V., and Chaturvedi, P. (2023). Design, control, reliability, economic and energy management of microgrid: a review. *e-Prime-Adv. Electr. Eng. Electr. Energy* 5:100239. doi: 10.1016/j.prime.2023.100239

Klir, G. J., and Yuan, B. (1996). Fuzzy sets and fuzzy logic: theory and applications. *Possib. Theory Probab. Theory* 32, 207–208.

Kumar, A., Ram, M., Goyal, N., Bisht, S., Kumar, S., and Pant, R. P. (2021). "Analysis of fuzzy reliability of the system using intuitionistic fuzzy set," in *Intelligent Communication, Control and Devices: Proceedings of ICICCD 2020* (Springer Singapore), 371–378. doi: 10.1007/978-981-16-1510-8_36

Kwasinski, A., Krishnamurthy, V., Song, J., and Sharma, R. (2012). Availability evaluation of micro-grids for resistant power supply during natural disasters. *IEEE Trans. Smart Grid* 3, 2007–2018. doi: 10.1109/TSG.2012.2197832

Li, H., and Yen, V. C. (1995). *Fuzzy Sets and Fuzzy Decision-Making*. London: CRC Press. ISBN: 978–0849389313

Li, W. (2013). *Reliability Assessment of Electric Power Systems Using Monte Carlo Methods*. Cham: Springer Science and Business Media.

Na, M. S., and Kim, J. O. (2019). Reliability evaluation of micro-grids containing PV system and hydropower plant. *Energies* 12:343. doi: 10.3390/en12030343

Nikos, H. (2007). Microgrids: an overview of ongoing research, development, and demonstration projects. *IEEE Power Energy* 5, 1349–1356. doi: 10.1541/ieejpes.129.1349

Onaolapo, A. K., and Ojo, E. E. (2023). "Effects of upside risk on microgrids' reliability considering the COVID-19 Pandemic," in *2023 31st Southern African Universities Power Engineering Conference (SAUPEC)* (IEEE), 1–6. doi: 10.1109/SAUPEC57889.2023.10057664

Pham, T. T., Kuo, T. C., and Bui, D. M. (2020). Reliability evaluation of an aggregate battery energy storage system in microgrids under dynamic operation. *Int. J. Electr. Power Energy Syst.* 118:105786. doi: 10.1016/j.ijepes.2019.105786

Ren, Y., Cui, B., Feng, Q., Yang, D., Fan, D., Sun, B., et al. (2020). A reliability evaluation method for radial multi-microgrid systems considering distribution network transmission capacity. *Comput. Industr. Eng.* 139:106145. doi: 10.1016/j.cie.2019.106145

Said, S. M., Aly, M., Hartmann, B., Alharbi, A. G., and Ahmed, E. M. (2019). SMES-based fuzzy logic approach for enhancing the reliability of microgrids equipped with PV generators. *IEEE Access* 7, 92059–92069. doi: 10.1109/ACCESS.2019.2927902

Santhan, K., Karuppiah, N., Praveen Kumar, B., Shitharth, S., and Dasu, B. (2022). Improvement of the resilience of a microgrid using fragility modeling and simulation. *J. Electr. Comput. Eng.* 2022:3074298. doi: 10.1155/2022/3074298

Talaat, M., Elkholy, M. H., Alblawi, A., and Said, T. (2023). Artificial intelligence applications for microgrids integration and management of hybrid renewable energy sources. *Artif. Intell. Rev.* 56, 10557–10611. doi: 10.1007/s10462-023-10410-w

Tazvinga, H., Thopil, M., Numbi, P. B., and Adefarati, T. (2017). "Distributed renewable energy technologies," in *Handbook of Distributed Generation: Electric Power Technologies, Economics and Environmental Impacts,* 3–67. doi: 10.1007/978-3-319-51343-0_1

Wesly, J., Brasil Jr, A. C., Frate, C. A., and Badibanga, R. K. (2020). Techno-economic analysis of a PV-wind-battery for a remote community in Haiti. *Case Stud. Chem. Environ. Eng.* 2:100044. doi: 10.1016/j.cscee.2020.100044

Wu, Z., and Xia, X. (2015). Optimal switching renewable energy system for demand side management. *Solar Energy* 114, 278–288. doi: 10.1016/j.solener.2015.02.001

Xu, X., Mitra, J., Wang, T., and Mu, L. (2016). Reliability evaluation of a microgrid considering its operating condition. *J. Electr. Eng. Technol.* 11, 47–54. doi: 10.5370/JEET.2016.11.1.047

Zimmermann, H. J. (2011). *Fuzzy Set Theory—and Its Applications*. New York: Springer Science and Business Media.

Nomenclature

λ_w, λ_{AD}, λ_{DA}, λ_{DD}, λ_{Bat}, λ_{cc} - are the failure rates of wind turbine generation, solar photovoltaic, AC/DC converter, inverter, DC/DC booster battery system, and charge controller, respectively.

λ_{ws}, λ_{pvs}, *and* λ_{bats} are the equivalent failure rate of wind, PV, and battery subsystems, respectively.

μ_{ws}, μ_{pvs}, *and* μ_{bats} are the equivalent repair rates of the wind, PV, and battery subsystems, respectively.

μ_w, μ_{AD}, μ_{DA}, μ_{DD}, μ_{Bat}, μ_{cc} are the repair rates of wind turbine generation, solar photovoltaic, AC/DC converter, inverter, DC/DC booster battery systems, and charge controllers, respectively.

Pup_{ws}, Pup_{pv}, Pup_{bat} are the probability of being at UP state in wind turbine generation, solar photovoltaic, and battery subsystem, respectively.

Pdn_{ws}, Pdn_{pv}, Pup_{bat} are the probabilities of being at a DOWN state in wind turbine generation, solar photovoltaic, and battery subsystems, respectively.

λ_{ew1}, λ_{ew2}, μ_{ew1} μ_{ew2} Pup_{ws1}, Pup_{ws2} Pdn_{ws1}, and Pdn_{ws2} are the equivalent failure rate, repair rate, availability, and unavailability fuzzy values of wind subsystem considering 5% of crisp value, respectively.

λ_{epv1}, λ_{epv2}, μ_{epv1}, μ_{epv2}, Pup_{pv1}, Pup_{pv2}, Pdn_{pv1}, andPdn_{pv2} are the equivalent failure rate, repair rate, availability, and unavailability fuzzy values of the PV subsystem considering 5% of crisp values, respectively.

λ_{eBat1}, λ_{eBat2}, μ_{eBat1}, μ_{eBat2}, Pup_{Bat1}, Pup_{Bat2}, Pdn_{Bat1}, and Pdn_{Bat2} are the equivalent failure rate, repair rate, availability, and unavailability fuzzy values of battery subsystem considering 5% of crisp values, respectively.